The Trace Element Chemistry of the Metal in IAB Iron Meteorites

John W. Larimer

Department of Geology and Center for Meteorite Studies, Arizona State University,
Tempe, AZ 85287, USA

Ermanno R. Rambaldi

Jet Propulsion Laboratory, California Institute of Technology, Pasadena, CA 91109

Z. Naturforsch. **44 a**, 968 – 978 (1989); received July 28, 1989

Dedicated to Heinrich Wänke on the occasion of his 60th birthday

Metal grains from a silicate inclusion in Landes, a group IAB iron-meteorite, were separated and analyzed via INAA for 14 siderophile elements. The same 14 elements were determined in matrix metal from Landes, 5 other IAB meteorites and three anomalous iron meteorites. Compared to the other samples and to chondritic metal, the inclusion metal is enriched in siderophile elements. In chondritic metal, the siderophile element contents are higher when Fe^0 is oxidized to FeO. Silicates in IAB inclusions contain little FeO, yet the metal is as rich in siderophile elements as the most oxidized chondrites.

Evidently the IAB body contained its full cosmic complement of S resulting in an FeS content ~5 × that of ordinary chondrites. This explains the composition of the metal since sulfurization, like oxidation, reduces the available Fe^0. IAB meteorites contain their full cosmic complement of other moderately volatile elements, which implies an equally high S content. A high S content significantly affects the melting and freezing of FeNi-metal. About 85% of the metal melts at the Fe-FeS eutectic (~960 °C), and all of the metal is molten at ~1050 °C. During cooling, ~85% of the metal crystallizes with a Ni content of $6 \pm 1\%$ between 1050° and 960 °C. Besides a small depletion in elements with low melting points or chalcophile tendencies this metal is little fractionated. Bellow 960 °C, the Ni content of the metal increases until the melt is exhausted. This Ni-rich metal also becomes progressively depleted in refractory elements and enriched in volatile elements. The crystallization process thus yields products that mimic the abundance and composition of group IAB meteorites.

Introduction

Heinrich Wänke first suggested to one of the co-authors (ERR) that the trace element contents of chondritic metal grains might provide clues to the origin and evolution of meteorites. Prof. Wänke suspected that some metal grains may retain a memory of nebular processes, while others may reflect secondary processes that occurred during reheating in the parent bodies. He further surmised that small, isolated grains are more likely to retain a record of primitive events while coarser grains that grew during reheating would record secondary processes. A study of metal grains extracted from chondrites and divided into different grain-size fractions was initiated and resulted in many important discoveries.

This study, which extends the work on chondritic metal, deals with the metal intermingled with a unique type of chondritic material: the silicate inclusions in IAB iron meteorites. IAB silicates contain most elements in chondritic proportions [1]. The inclusions are embedded in massive matrix metal which texturally, but not chemically, resembles other more typical iron meteorites. The inclusions' shapes range from angular to well-rounded and the sizes range from several cm to a few mm. Their mineralogy is typically chondritic: olivine, pyroxene and plagioclase are dominant. The IAB silicates differ from chondrites in two important aspects, however: their FeO contents indicate an oxidation level between tht of E- and H-chondrites and they contain less FeS and metal than most chondrites [2].

Iron meteorites are classified on the basis of the Ni, Ga, Ge and Ir contents of their matrix metal [3]. The Ga and Ge contents are higher and the Ni contents vary over a wide range (5 to 25%) in Group IAB than in any other group of iron meteorites. Correlations between these diagnostic elements in Group IAB, such

---

Reprint requests to Dr. J. W. Larimer, Department of Geology, Arizona State University, Tempe, AZ 85287, USA.

0932-0784 / 89 / 1000-0968 $ 01.30/0. – Please order a reprint rather than making your own copy.

as Ir to Ni, as well as correlations among other elements, distinctly differ from correlations between the same elements in other iron meteorite groups [4]. Nearly half of the 100 or so IAB iron meteorites contain silicate inclusions [3]. Interestingly, the volatile element/Ni ratios in IAB meteorites with the highest volatile contents resemble those in CI chondrites.

In the metal of IAB meteorites with 7–15% Ni, the Widmanstätten patterns and Ni diffusion profiles are similar to those in typical octahedrites. (The Widmanstätten pattern is not well developed in IAB meteorites that have <7% or >15% Ni, just as observed in all other iron meteorites.) Similar Ni diffusion profiles suggest similar cooling rates. Recent diffusion rate data [5], indicate cooling rates on the order of 25°/Myr, a value consistent with cooling rate estimates based on fission track studies of the silicates [6, 7 and Pellas, pers. comm.]. This implies burial depths of 50–75 km in a body with the chemical and physical properties of chondrites.

Radiometric dating of the silicate inclusions, based on Rb/Sr and ^{40}Ar/^{39}Ar, indicate ages on the order of 4.55 ± 0.1 Byr [8, 9]. The silicates also contain "planetary" noble gases (see e.g. [10]) and excess ^{129}Xe, which correlates with Ni content in a manner suggesting that the Ni-rich members are older than the Ni-poor members [11]. The ^{40}Ar/^{39}Ar plateaus are well defined, except in Copiapo, the only meteorite studied that displays signs of modest shock.

This evidence indicates that IAB meteorites formed early in the history of the solar system and have remained relatively unaltered. Models for the origin of these meteorites fall into two categories: primary models, which invoke nebular processes, and secondary models, which hypothesize differentiation in a parent body. Both models regard the silicate chemistry and mineralogy as primitive, reflecting local nebular conditions, like those commonly invoked to explain chondrites (e.g., local variations in oxidation state and oxygen istotope composition [12]). The models differ in the way they explain the fractionated matrix metal composition.

In primary models, the metal and silicates accrete as solids. This avoids the problem of rapid unmixing of silicates and molten metal [13]. Several nebular fractionation processes are required to explain the trace element patterns in the matrix metal: loss of a large fraction of refractory siderophiles; removal of Fe via oxidation, sulfurization or some unknown process; remixing refractory and volatile elements in such a way that the refractories decrease and the volatiles increase with increasing Ni content [14].

In secondary models, where IAB meteorites are thought to form in a parent body, the matrix metal would be a product of the differentiation process by which cores are formed. The IAB meteorites might represent samples of the core-mantle boundary [15], fractional crystallization of an S-rich melt [16, 17], or an arrested stage of core formation (i.e., as the molten metal sank through the mantle it crystallized prematurely and trapped the silicates [18]). If the metal froze prior to core formation, then its composition might reflect partial melting where the elemental abundance patterns differ markedly from those produced by fractional crystallization.

In considering secondary models, the existence of a small group of related meteorites, sometimes referred to as winonaites, cannot be ignored. These are stony meteorites whose elemental and O-isotopic composition and silicate oxidation level are similar to IAB silicate inclusions [19–22]. Though these meteorites resemble ordinary chondrites in many respects, they do not fall into any of the recognized groups. The differences include: no chondrules have been observed, a distinct O-isotopic composition and higher contents of moderately volatile elements, including S in some cases.

One purpose of our study was to see what, if any, relationship might exist between the small metal grains in the silicate inclusions and the surrounding matrix metal. Conceivably the metal in the inclusions might reflect the composition of the residual solid metal in a partial melting process. On the other hand, it might provide some insights into the complex nebular fractionation processes which may be responsible for the matrix metal compositions. Or it could have the same composition as the matrix metal, implying complete equilibration. Previous studies on the composition of inclusion metal are limited to rather incomplete microprobe analyses or inferences based on bulk analyses and an assumed metal content [1, 23].

Analytical Procedure

The silicate inclusions in the IAB meteorite Landes appeared visually to contain more metal than the other meteorites examined. Metal from these inclusions was extracted, split into grain size fractions and analyzed. As a comparison, we analyzed the matrix metal from

Table 1. Analyses of matrix metal.

Meteorite	Ni %	Co ppm	Cu ppm	Ga ppm	Ge ppm	As ppm	Ru ppm	Sb ppm	W ppm	Re ppm	Os ppm	Ir ppm	Pt ppm	Au ppm
IAB														
Landes	6.5	4590	330	99	440	9.6	10.4	0.27	1.6	0.41	4.9	4.6	12.8	1.3
Paracutu	7.5	4630	140	84	283	14.4	6.2	0.44	2.0	0.29	3.3	3.0	11.8	1.5
Four Corns.	9.0	4650	210	51	156	14.2	2.4	0.40	0.5	0.23	2.5	2.4	7.7	1.4
Woodbine	10.0	5030	200	41	89	13.9	2.5	0.64	0.4	0.14	2.2	2.0	2.6	1.4
Pitts	11.9	5300	390	35	78	15.1	–	1.01	0.4	–	–	1.1	–	1.5
	11.8	5430	430	35	97	17.3	1.9	1.09	0.3	0.10	1.3	1.2	2.0	1.5
Persimmon creek	12.7	5170	290	32	55	13.3	1.3	0.84	0.7 *	–	–	0.9	–	1.2
	12.9	5420	350	32	44	13.5	–	0.83	0.2	0.06	0.9	0.9	1.7	1.3
Anomalous														
Zacatecas	5.8	4540	120	76	270	5.3	9.1	0.11	1.6	0.11	2.4	2.2	13.9	0.6
Morradal	18.1	7090	440	44	103	7.9	–	0.25	0.5	0.08	1.3	0.7	5.1	1.0
Butler	14.3	11700	130	86	1692	39.0	38.0	0.44	4.5	0.18	3.7	1.8	49	5.3

Table 2. Trace element contents of metal from Landes silicate inclusions.

Size fract. mesh	Ni %	Co ppm	Cu ppm	Ga ppm	Ge ppm	As ppm	Ru ppm	Sb ppb	W ppm	Re ppb	Os ppm	Ir ppm	Pt ppm	Au ppm	Cr ppm	Mn ppm
>200	10.5	3420	1280	133	537	9.8	16.8	452	1.86	550	7.1	8.6	20.3	2.14	–	–
200–325	13.0	2880	2420	170	760	11.2	19.0	620	2.06	832	8.9	8.3	30.7	2.54	–	–
<325	13.7	2320	3540	190	645	12.3	22.7	1360	2.70	570	10.6	9.4	21.0	2.81	–	–
Bulk metal	11.2	3220	1700	145	586	10.3	17.7	570	1.97	600	7.7	7.3	22.2	2.27	–	–
Silicates without metal	790 ppm	27.5	–	–	–	–	–	–	–	–	435 ppb	135 ppb		24 ppb	1230	2300

Landes, five other IAB meteorites, and three anomalous iron meteorites for the same suite of elements.

Several small chips (~35 g) of material were removed with a steel chisel from the center of a relatively large silicate inclusion in Landes. These chips were crushed in a steel mortar and gently ground in an agate mortar. Using 200- and 325-mesh sieves, this finely ground material was separated by grain-size into three fractions: (1) coarse, >200 mesh; (2) intermediate, 200–325 mesh; and (3) fine, >325 mesh. The metal grains in each fraction were separated using a hand magnet, gently crushed again to remove adhering silicates, washed in acetone and examined microscopically to assure purity. An aliquot of 100–200 mg of each fraction was separated for analyses.

Small chips of the matrix metal samples were removed (400–500 mg) from a larger piece of the meteorite with a diamond saw. Each sample was placed in dilute nitric acid for several minutes to remove surface contaminants; subsequent microscopic examination revealed no evidence of dissolution, such as etch pits.

The samples were irradiated (7×10^{11} n/cm^2 sec) in the TRIGA-reactor at the University of Mainz and counted in a large volume Ge(Li) detector, using the standards and procedures routinely employed [24]. Computer analyses of the Y-spectra permitted resolution of interferring peaks, such as Os on As.

The procedures followed Rambaldi's study of chondritic metal [25, 26], in which the results agreed closely with previous studies. The precision of the method differs among the elements; the 2σ uncertainties based on counting statistics are: Co, Ir, Ni and Os, ±5%; As, Au, Re and W, ±10%; Cu, Pt, and Ru, ±20%. All samples are from the Nininger collection at Arizona State University except Landes, which is from the Max-Planck-Institut für Chemie in Mainz.

Results

The measured concentrations of 16 elements are shown in Tables 1 and 2. Table 2 also contains addi-

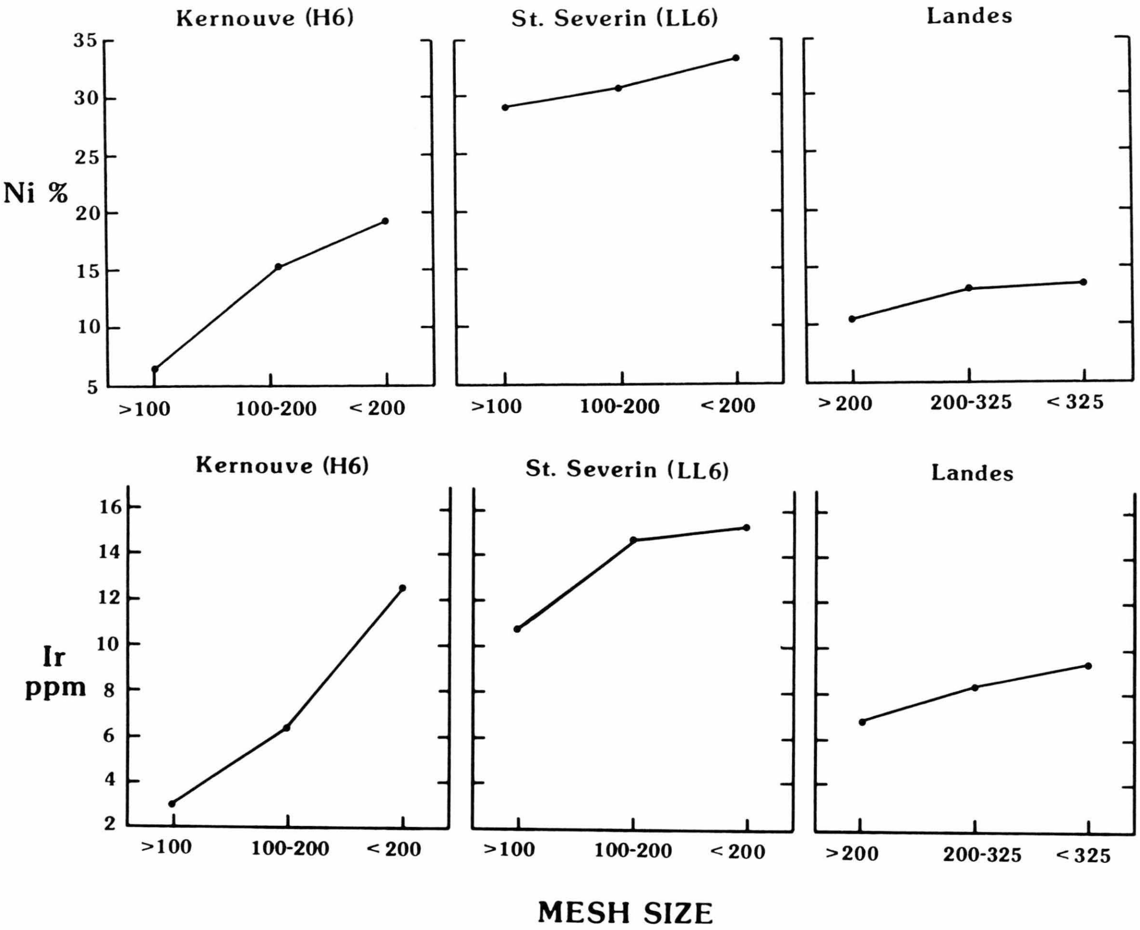

Fig. 1. In Landes inclusion metal, as in chondrites, element concentrations vary with grain size, generally increasing with decreasing grain size. In chondrites, the differences in composition between coarse- and fine-grain size decrease with increasing petrographic type. The difference in Landes inclusion metal is less than in Type 6 condrites.

tional data on a few elements measured in the silicate fraction of Landes after the metal had been extracted; their concentrations indicate that about 99% of the metal was removed. The total mass of the metal in this particular sample of inclusion material was 5.73 wt%. The elemental concentrations in the bulk metal were calculated from the mass of the three grain-size fractions (Table 2).

Discussion

Inclusion metal. The concentrations of Ir and Ni in the three grain-size fractions of metal extracted from the silicate inclusion in Landes are compared to similar data from two chondrites in Figure 1. Elemental concentrations in Landes metal, like those in chondrites, generally increase with decreasing grain size.

In chondrites, the systematic variation in metal composition is attributed to the combined metamorphic effects of grain coarsening and element redistribution and homogenization of the grains. This interpretation is based on the observations that, with increasing metamorphic grade, the amount of fine-grained metal decreases and the difference in composition between fine- and coarse-grained matal decreases. The interpretation also explains two exceptions to the general compositional trend: Co and Fe, which tend to concentrate in the coarser kamacite grains [25, 26]. Since the difference in composition between the coarse- and fine-grain size fractions is less in Landes than in typical type 6 chondrites, the inclusion metal appears to be more equilibrated than the most strongly metamorphosed chondrites.

Several conclusions can be drawn from these data. First, the inclusion metal appears to retain some memory of a more primitive state. It has not completely equilibrated although it is more equilibrated than the metal in petrographic type 6 chondrites. Second, the metal grains extracted from the inclusion are not simply fragments of the surrounding matrix metal incorporated by accident into our samples. And finally, it appears that the metal in the inclusion and the matrix metal did not equilibrate implying incomplete element exchange between matrix and inclusion metal.

Matrix metal. Figure 2 summarizes the compositional data for the six IAB meteorites studied as well as the data on the composition of the bulk metal in the inclusion. For comparative purposes, the data have been normalized to C1 and Co, the least fractionated element in IAB meteorites. Similar data on San Cristobal [14], an IAB meteorite that is more Ni ricch (25%) than any we studied, are also plotted. The data on the three anomalous meteorites do not fall into any consistent pattern and will not be further discussed here.

The general compositional trends in IAB meteorites are readily evident in the data: Landes, with the lowest Ni content has the lowest volatile (Sb, As and Au) contents and the highest Ga, Ge and refractory element contents. Conversely, San Cristobal, with the highest Ni content has the highest volatile contents and the lowest Ga, Ge and refractory element contents. In addtion, several systematic trends sugget a common fractionation process; e.g., Ge/Ga and Pt/Ga ratios gradually change from values >1 in Landes to <1 in San Cristobal.

Comparison of matrix and inclusion metal. The compositions of the inclusion and matrix metal are compared in Figure 2. The inclusion metal is enriched in all elements relative to all other samples except for San Cristobal, where the volatile elements are slightly more enriched. The pattern among the elements in the inclusion metal is quite similar to the pattern found in the matrix metal of Landes.

To put the composition of the matrix and inclusion metal into a broader context, and to better understand the origin of IAB meteorites, we have compared the matrix and inclusion data from Landes with chondritic metal [25, 26] in Figure 3. For the elements plotted, the concentrations in the inclusion metal are similar to, or higher than, the concentrations of the same elements in metal from L- and LL-chondrites. The composition of the matrix metal yields a parallel trend, displaced to lower concentrations by a factor of about 0.6.

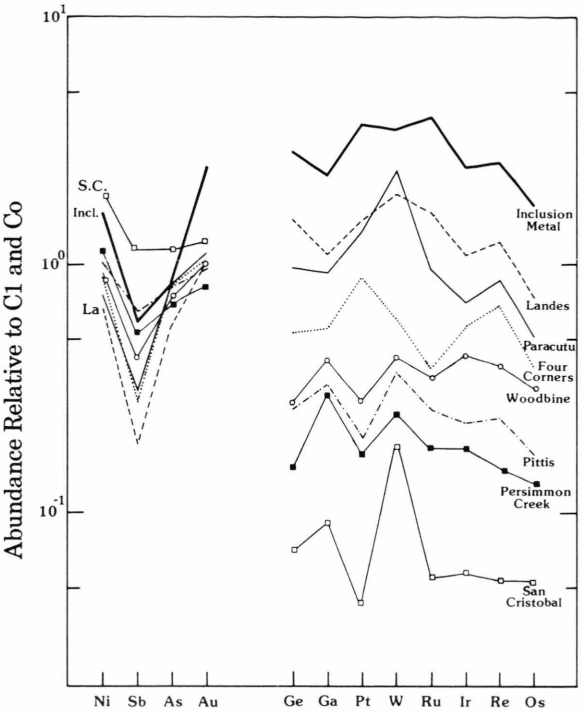

Fig. 2. Minor and trace element contents in IAB matrix metal vary in a systematic way: with increasing Ni content the Ga, Ge and refractory element contents decrease and the volatile element contents increase.

The most interesting feature of the inclusion metal is the high concentration of all siderophile elements. Among chondrites, siderophile elements are most enriched in metal in LL chondrites owing to their low metal content. LL chondrites contain only a few per cent metal because they have low total Fe and comparatively large FeO contents. IAB meteorites, however, have high total Fe contents and the silicate inclusions have relatively low FeO contents (or FeO/FeO + MgO ratios).

The dashed line in Fig. 3 illustrates the calculated siderophile contents in metal from a body that has H-group abundances of siderophiles but whose silicates are reduced to the level observed in IAB inclusions. Obviously, the Fe^0 generated by the reduction of FeO decreases, rather than increases, the concentration of siderophile elements in the metal. This observation raises the question of why the elemental concentrations are so high in the inclusion metal.

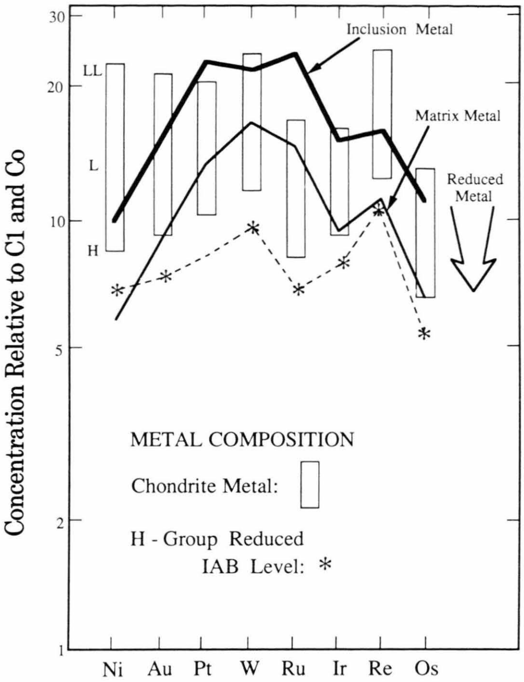

Fig. 3. Siderophile element contents in Landes inclusion metal are as high, or higher, than in L- and LL-group metal. High siderophile contents in chondritic metal are related to high FeO contents in silicates. The siderophile element contents in metal from a body whose FeO content is reduced to the level observed in IAB silicate inclusions (dashed line) are lower than H-group metal, not higher than L- or LL-group metal.

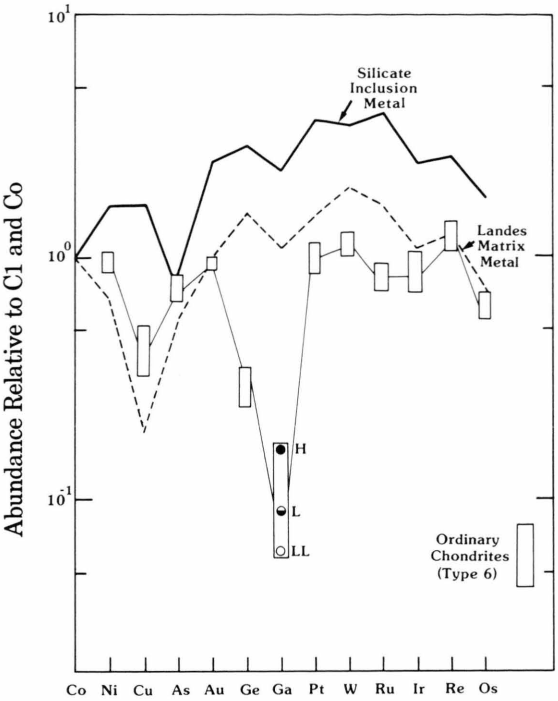

Fig. 4. Volatile siderophile elements (As, Au, Cu, Ga and Ge) which, along with S, are depleted in ordinary chondrites are not depleted in inclusion metal.

There are two possible explanations: either the body's total iron content was exceedingly low or a significant fraction of the iron was tied up in another phase. The evidence from chondrite makes a low total iron content an improbable explanation. Low total Fe contents in chondrites are always accompanied by low abundances of all non-volatile siderophile elements. In ordinary chondrites all elements shown in Fig. 3 increase or decrease in abundance along with Fe, Ni and Co [27]. The high concentrations of siderophile elements in metal from L- and LL-relative to H-chondrites is due almost entirely to the larger fraction of Fe present as FeO in L- and LL-chondrites.

In planetary material, most of the Fe is found in metal, silicates (as FeO) and FeS. In order to reduce the fraction of Fe in the metal, the fraction present as FeO or FeS or both would have to increase. Since the silicates contain less FeO than ordinary chondrites, the high siderophile contents in the inclusion metal suggest an enhanced FeS content. The required FeS content, though seemingly high, is plausible and consistent with other evidence.

The solar abundance of S is more than half of Fe; hence, if a body acquires its full complement of S then a large fraction of its Fe will be present as FeS. Ordinary chondrites did not acquire their full solar complement of S; about 75% along with a similar amount of the other moderately volatile elements seems to be missing.

In contrast to ordinary chondrites, IAB meteorites are comparatively rich in S and are not depleted in moderately volatile elements. This is illustrated in Fig. 4 which compares the siderophile element abundances in the inclusion metal to chondritic abundances. Elements that are depleted in chondrites along with S: Au, Cu, Ga and Ge, are not depleted in the inclusion metal. Several lines of evidence thus indicate that the IAB body acquired its full solar complement of S.

Implications of an S-rich IAB parent body. If we assume that the IAB parent body contained its full solar complement of S and other non-volatile elements, then it is possible to calculate the proportions

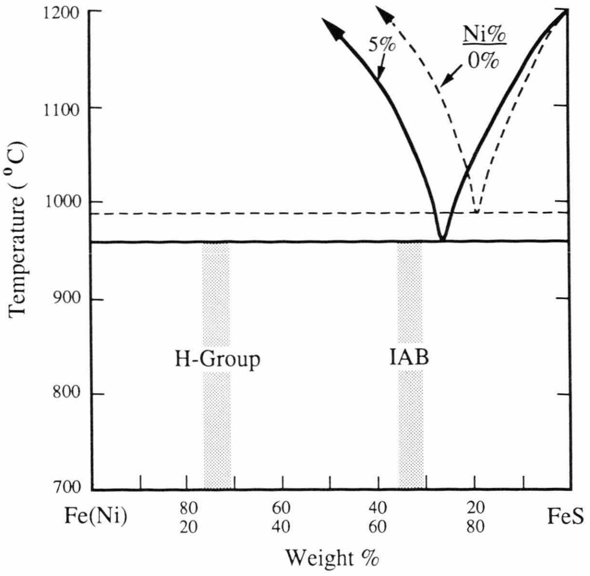

Fig. 5. A S-rich IAB body lies much closer to the eutectic composition in the Fe-FeS system than an S-depleted ordinary chondrite body. In an IAB body, with an FeO content commensurate with that of IAB inclusions, and with solar proportions of Fe, Ni and S (Ni = ~4.5 wt%), all FeS and about 85% of the FeNi-metal melts at the eutectic. In contrast, in an H-group body all FeS but only 30% of the FeNi-metal melts. The dashed and solid lines indicate the eutectic relations at 0 and 5 wt% Ni, respectively.

Table 3. Comparison of estimated IAB parent body composition with chondrites.

	IAB	H-Group	L-Group
SiO_2	34.67	36.17	39.49
MgO	24.73	22.93	24.55
FeO	2.83	9.26	14.97
Fe	10.74	17.76	7.04
Ni	1.61	1.68	1.06
FeS	25.42	5.69	5.77
Total Fe	27.00	28.58	22.32
For the Fe-Ni-S system			
Fe	73.13	85.07	77.22
Ni	4.37	6.69	7.64
S	22.50	8.24	15.14

of the major species in the body (Table 3). The FeS wt% in such a body is nearly 5 × that found in the ordinary chondrites. This amount of FeS has important effects on the melting and freezing relations that are central the chemical history of metallic melts.

Figure 5 is a simple binary (0% Ni), or pseudobinary (5% Ni), in the Fe-Ni-S system and is useful for comparing the melting and freezing relations in an S-rich IAB body with those in an ordinary (H-group) chondrite body. The key difference is that the calculated IAB composition falls much closer to the eutectic than H-group composition. Adding about 5% Ni lowers the melting temperature and shifts the "eutectic" composition even closer that of the IAB body. These relations would, of course, change slightly if the presence of other important minor components (e.g., C and P) were taken into account.

The S content of a body plays an important role throughout the core forming process; from melting to gravitational segregation to crystallization. During heating, the S content determines the proportion of metal (or FeS) that melts at the eutectic temperature. In a body with H-group composition, all of the FeS and 30% of the metal would melt at the eutectic. By contrast, in the IAB body, all of the FeS would also melt at the eutectic but, far more important, ~85% of the metal would melt as well. With further heating, the remaining metal would gradually melt. However, in the H-group body the metal would melt over a 500° interval, whereas the metal in a IAB body would completely melt within a 100° interval.

These 500° and 100° intervals apply if the liquid and metal remain in contact during melting. On a dynamic system, the dense liquid would drain off once sufficient melt had formed to reduce the supporting rock strength to the point where gravitational forces take effect. In an H-group body, draining off the liquid would extend the melting interval slightly, to about 520°. The situation would be different in the IAB body where a large fraction of the whole rock melts at the eutectic (~35 wt% compared to ~10 wt% in an H-group body). This would lower the rock strength and drastically increase the rate at which molten globules would grow in size. A combination of lowered rock strength and massive molten globules may allow the melt, bearing all of the S, to drain off rapidly leaving behind only a few isolated metal grains in the silicates. These metal grains would not melt until the temperature reached the melting point in an S-free system, 1450–1500 °C. Perhaps this explains why metal grains remain in the silicate inclusions. Taylor [28] has attempted to calculate the rate at which molten metal-sulfide would segregate from silicates and concludes that a large degree of partial melting and large globules are necessary to render the process efficient. However, this conclusion is based in part on melting experiments of L chondrites, whose metal plus sulfide

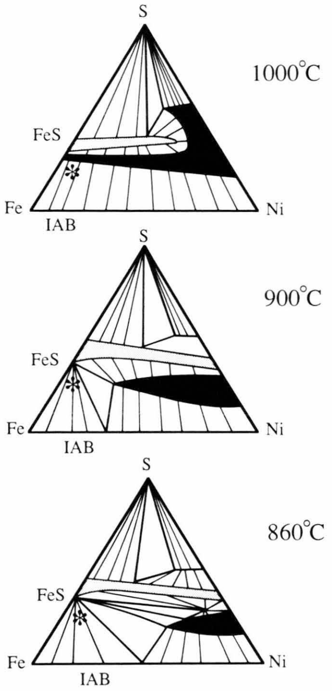

Fig. 6. The crystallization history of a melt with the Fe, Ni and S contents of the IAB body (*) can be followed in the Fe-Ni-S system [29]. The first metal to crystallize (~1050 °C) contains 6±1 wt% Ni. Metal with this composition continues to crystallize, and the coexisting melt changes composition along the tie line toward the melt field, as the temperature falls to ~960 °C. At ~960 °C, when nearly 85% of the FeNi-metal will have crystallized, the shrinking liquid field moves to the right across the tie line. At lower temperatures, the melt becomes progressively enriched in S and Ni and the crystallizing metal becomes more Ni-rich until melt is exhausted.

contents are even lower than in H chondrites which have much lower metal plus sulfide contents than those contemplated here.

The freezing relations are also quite different. In an H-group body, the melt begins to crystallize at relatively high temperatures, 1450–1500 °C, depending on the proportions of S, P, C, Fe and Ni. Fractional crystallization in the solidifying core gives rise to the chemical trends observed in most iron meteorite groups, as first suggested by Scott [14]. In the IAB body, however, crystallization would begin at much lower temperatures, ~1050 °C, and the fractional crystallization trends would be quite different.

Crystallization relations in the IAB body can best be followed by considering the Fe-Ni-S system (Figure 6). Let us assume that the melt's original bulk composition was acquired by melting all of the metal and sulfide in the body (Table 3). The compositional relationships between this original melt and the first metal to precipitate are shown at 1000 °C in Figure 6. The original composition lies in a region of the system where the tie lines between liquid and solid are almost parallel to the Fe-S side of the triangle. If the tie lines were parallel, the original melt and coexisting solid would have the same Ni content. However, from Kullerud's [29, pers. comm.] working diagrams, where the end points of the tie lines can be read more accurately, the tie lines are not exactly parallel to the Fe-S boundary. The first metal to precipitate actually is slightly enriched in Ni, 6±1 wt% relative to ~4.50 wt% in the original melt.

There is an importance difference between the crystallization process at these temperatures and compositions and the process normally envisioned for other groups of iron meteorites. Within experimental uncertainty [29], it appears that there is little change in the composition of the precipitating solid between the onset of crystallization at 1050 °C and 960 °C, less than ±1% or so. This relationship results from the fact that the orientation of the tie lines between liquid and solid does not change appreciably over this temperature interval. Consequently, between 1050 and 960 °C the proportion of crystalline metal to melt changes markedly but its composition remains constant.

Thus, as crystallization proceeds, metal with 6±1 wt% Ni cotinues to precipitate as the composition of the liquid shifts toward the intersection of the tie line with the liquid field. At about 960 °C, the tip of the liquid field, which is shrinking in size and pulling away from the Fe-S boundary, passes through the pertinent tie line. (The liquid field has shrunk to an even smaller size in the 900 °C diagram in Figure 6.) The relations at 960 °C can also be ascertained from the pseudo-binary drawn for ~5 wt% Ni in Figure 5. In effect, the "eutectic" in this pseudo-binary is encountered at 960 °C. As the temperature falls below 960 °C, FeS would begin to precipitate along with metal. The composition of both the metal and coexisting liquid now begins to change, shifting toward higher Ni contents (see the 900 °C and 860 °C diagrams in Figure 6).

It is of interest to consider the proportion and composition of the metal that crystallizes above and below 960 °C. The proportion of the metal that would crystallize above this temperature is similar to the proportion that melts at the eutectic during the heating part of the cycle, about 85%. Thus, about 85% of the metal in a system with the composition of our IAB body should crystallize with 5–7 wt% Ni. The remaining 15% would crystallize at lower temperatures and contain greater amounts of Ni.

Some comparisons with IAB iron meteorites. Viewed as a group, IAB meteorites display many characteristics that are consistent with the melting-freezing relations just discussed. In terms of numbers, the Ni contents in the vast majority of IAB meteorites cluster around 6 wt% Ni, and there is a sparsely populated tail with higher Ni contents. This is consistent with the proportion and composition of recrystallized metal in our hypothetical, S-rich IAB parent body.

Kracher [16] proposed a similar origin and attempted to explain the trace element concentrations in terms of fractional crystallization from an S-rich melt. Unfortunately, the only experimental data available were obtained at much higher temperatures than those contemplated by Kracher or us falling in the 1250–1495 °C range [30–32]. These studies did show that adding S to metal-rich melts at high temperatures would affect the metal/liquid distribution coefficients in a significant way. But it is unlikely that the quantitative values obtained can be extrapolated to the compositions and temperatures of interest here. Kracher adopted a semi-empirical approach and adjusted the distribution coefficients to match the concentration patterns observed in IAB meteorites. The values he obtained are plausible, although the model adopted in deriving the values can not be correct.

At pressent, it is only possible to draw some broad generalizations. The more refractory siderophiles, along with Ga and Ge, almost certainly are concentrated in the first crystals to form. But since the Fe and Ni contents of the metal are not expected to change appreciably during the first 85% of the crystallization process, the proportions of these elements are unlikely to change much either. It is only during crystallization of the last 15% of the original melt when these elements will show a decrease with increasing Ni content.

On the other hand, elements with low melting points (As, Au, Cu and Sb) can be expected to be more concentrated in the melt throughout the crystallization process. Again, however, the extent of fractionation will be suppressed because such a large fraction of the metal will crystallize with the same Fe and Ni contents. Elements with stronger chalcophile tendencies (e.g., Sb) are likely to be more highly concentrated in the S-rich melt and to display somewhat greater fractionation. These generalization on elements with either high or low melting poi.nts are consistent with the patterns found in IAB meteorites (Table 1 and Figure 2).

Summary and Implications

Metal grains from the chondritic silicate inclusions in IAB meteorites contain high concentrations of siderophile elements compared to metal grains in ordinary chondrites. The silicates in IAB inclusions are more reduced than H-group chondrites indicative of less FeO, and more available Fe. But to form metal with high siderophile element contents requires less available Fe, not more. This dilemma can be resolved plausibly by assuming that the IAB body contained its full solar complement of S. The FeS content of such a body would be about 5 times that of ordinary chondrites, which do not contain their full cosmic complement of S. The metal in this hypothetical IAB body would be enriched in siderophiles to about the level found in the metal grains from the silicate inclusions.

A high S content is also consistent with the observation that other moderately volatile elements, which are depleted in ordinary chondrites by similar factors of 0.2–0.3 relative to solar abundances, are present in solar proportions in IAB meteorites. The IAB body thus appears to differ from ordinary chondrites in that the moderately volatile elements are not depleted.

It is also of interest to consider the winonaite meteorites, which may represent samples of the mantle of the body in which the IAB meteorites formed. They too contain nearly their full cosmic complement of moderately volatile elements and several contain large amounts of FeS [21]. One, Pontlyfni, in the sample studied contains 18.8% FeS and 23.9% FeNi, although Graham et al. [20] note that these phases are not distributed uniformly. The siderophile element content of the metal, inferred from a bulk analysis [19], is high though not as high as that found here in the metal from Landes.

A high S content in the IAB body would cause most of the metal to melt and freeze over a relatively narrow temperature range, 960 to 1050 °C. Fractional crystallization within this temperature range produces little variation in composition. Nearly 85% of the solidified metal will contain 5–7 wt% Ni, and its minor and trace element contents will be lower but will be present in more or less the same proportions as in the pre-existing solid grains. The remaining 15% of the metal should, however, display large variations in composition resulting from fractional crystallization. With increasing degree of crystallization, the Ni content and the content of elements with low melting points will increase while the Ga, Ge and refractory element contents will decrease. Quantitative estimates must await additional experimental data, but qualitatively the predicted patterns match those observed in IAB matrix metal.

It may be significant that many features in IAB meteorites can be explained if the highest temperature experienced was less than 1150 °C and the entire melting and freezing cycle occurred in the 900° to 1150 °C interval. At temperatures higher than 1150 °C the silicates would begin to melt and lose their chondritic composition. In some cases the silicates appear to have just begun to melt; in Campo del Cielo and Landes the silicate inclusions display slightly fractionated REE patterns suggesting a small degree of partial melting [H. Palme, pers. comm.]. The lower limit is set by the temperature at which kamacite becomes stable (<910 °C). If the metal had crystallized as a two phase mix of kamacite and taenite then the Widmanstätten pattern would not develop.

Such low formation temperatures for iron-rich meteorites eases the problems associated with the retention of noble gases in the silicate inclusions. Moreover, the Ni rich members could have evolved at the lowest temperatures, and retained more gases, if they are the product of interactions between the Ni- and S-rich melt and the surrounding chondritic mantle rocks. This provides a simple explanation for the correlation between excess ^{129}Xe and Ni content since high Ni contents would be indicators of low formation temperatures.

IAB meteorites could thus have formed in a S-rich core, or near the core mantle boundary ar relatively low temperatures. The segregation of solid silicates from such a core would be more sluggish than in normally envisioned high temperature cores. Moreover, at the core solidified, the brittle solid mantle would presumably collapse in response to the decrease in volume opening fractures that would be filled by the last, most S-rich molten metal to crystallize.

A comparatively S-rich parent body accounts for most features of IAB meteorites in a more straightforward manner than models invoking nebular fractionation. Some ineresting problems remain, however. As Kracher [16] suggested the high Ni members of Group IAB are best explained as crystallizing during FeS precipitation. But if this is correct, eutectic intergrowths of FeS and metal would be expected and these are not observed. We can speculate that the FeS is sequeezed, or filter pressed, out of the crystallizing metal into zones of weakness. This might help explain the other problem; having invoked a high S content it is necessary to explain the lack of FeS-rich meteorites. This, of course, is a long standing problem in meteorites. We have little to add to the suggestions of Kracher and Wasson [33] who appeal to FeS friability during breakup and exposure and the reactivity of FeS in the terrestrial environment which limits its survival on earth.

Acknowledgements

The help of the staff at the TRIGA reactor in the Institut für Kernchemie at the University of Mainz is gratefully acknowledged. Portions of the work were supported by NASA Grant 7074 and the Deutsche Forschungsgemeinschaft. We also thank E. R. D. Scott for helpful review.

[1] R. W. Bild, Geochim. Cosmochim. Acta **41,** 1439 (1977).
[2] T. E. Bunch, K. Keil, and E. Olsen, Contrib. Mineral. Petrol. **25,** 297 (1970).
[3] E. R. D. Scott and J. T. Wasson, Rev. Geophys. Space Phys. **13,** 527 (1975).
[4] E. R. D. Scott, Geochim. Cosmochim. Acta **36,** 1205 (1972).
[5] V. Saikumar and J. I. Goldstein, Geochim. Cosmochim. Acta **52,** 715 (1988).
[6] Y. Benheiri, P. Pellas, and D. Storzer, Icarus **40,** 497 (1979).
[7] Y. Benkheiri, Meteoritics **19,** 188 (1984).
[8] D. S. Burnett and G. J. Wasserburg, Earth Planet. Sci. Lett. **2,** 397 (1967).
[9] Niemeyer, S., Geochim. Cosmochim. Acta **43,** 1829 (1979).
[10] D. Bogard, D. Burnett, P. Eberhadt, and G. J. Wasserburg, Earth Planet. Sci. Lett. **3,** 275 (1968).
[11] Niemeyer, S., Geochim. Cosmochim. Acta **43,** 8943 (1979).
[12] R. N. Clayton, N. Onuma, and T. K. Mayeda, Earth Planet. Sci. Lett. **30,** 10 (1876).
[13] R. A. Fish, G. G. Goles, and E. Anders, Astrophys. J. **132,** 243 (1960).
[14] E. R. D. Scott and R. W. Bild, Geochim. Cosmochim. Acta **38,** 1379 (1974).
[15] B. Mason, Mineral. Mag. **36,** 120 (1967).
[16] A. Kracher, Geophys. Res. Lett. **9,** 412 (1982).
[17] A. Kracher, Proc. 15th LPSC, J. Geophys. Res. **90,** C689 (1985).
[18] W. R. Kelly and J. W. Larimer, Geochim. Cosmochim. Acta **41,** 93 (1977).

[19] A. M. Davis, R. Gananathy, and L. Grossman, Earth Planet. Sci. Lett. **35,** 19 (1977).
[20] A. L. Graham, A. J. Easton, and R. Hutchison, Min. Mag. **41,** 205 (1977).
[21] H. Palme, L. Schultz, B. Spettle, H. W. Weber, H. Wänke, M. Chistophe Michel-Levy, and J. C. Lorin, Geochim. Cosmochim. Acta **45,** 727 (1981).
[22] L. Schultz, H. Palme, B. Spettle, H. W. Weber, H. Wänke, M. Chistophe Michel-Levy, and J. C. Lorin, Earth Planet. Sci. Lett. **61,** 23 (1982).
[23] A. Kracher, Proc. 18th LPSC, J. Geophys. Res. **93,** C 485 (1988).
[24] H. Wänke, H. Kruse, H. Palme, and B. Spettel, J. Radioanal. Chem. **38,** 363 (1977).
[25] E. R. Rambaldi, Earth Planet. Sci. Lett. **31,** 224 (1976).
[26] E. R. Rambaldi, Earth Planet. Sci. Lett. **36,** 347 (1977).
[27] J. W. Larimer and E. Anders, Geochim. Cosmochim. Acta **34,** 367 (1970).
[28] G. J. Taylor, Lunar and Planet. Sci. **XX,** 1109 (1989).
[29] G. Kullerud, Carnegie Inst. Wash. Yearbook **62,** 175 (1963).
[30] J. I. Goldstein and J. J. Friel, Proc. Lunar Planet. Conf. 9th, **1978,** p. 1423.
[31] J. Willis and J. I. Goldstein, Proc. Lunar Planet. Conf. 13th Part 1. J. Geophys. Res. **87** (Suppl.) A 435 (1982).
[32] J. H. Jones and M. J. Drake, Geochim. Cosmochim. Acta **47,** 1199 (1983).
[33] A. Kracher and J. T. Wasson, Geochim. Cosmochim. Acta **46,** 2419 (1982).